J Appl Physiol 125: 1720–1730, 2018.
First published September 6, 2018; doi:10.1152/japplphysiol.00487.2018.

RESEARCH ARTICLE

The spatial pattern of methacholine bronchoconstriction recurs when supine independently of posture during provocation but does not recur between postures

Eric T. Geier,[1] Kent Kubo,[1] Rebecca J. Theilmann,[2] Gordon K. Prisk,[1] and Rui C. Sá[1]

[1]*Department of Medicine, University of California, San Diego, California; and* [2]*Department of Radiology University of California, San Diego, California*

Submitted 1 June 2018; accepted in final form 4 September 2018

Geier ET, Kubo K, Theilmann RJ, Prisk GK, Sá RC. The spatial pattern of methacholine bronchoconstriction recurs when supine independently of posture during provocation but does not recur between postures. *J Appl Physiol* 125: 1720–1730, 2018. First published September 6, 2018; doi:10.1152/japplphysiol.00487.2018.—The location of lung regions with compromised ventilation (often called ventilation defects) during a bronchoconstriction event may be influenced by posture. We aimed to determine the effect of prone versus supine posture on the spatial pattern of methacholine-induced bronchoconstriction in six healthy adults (ages 21–41, 3 women) using specific ventilation imaging. Three postural conditions were chosen to assign the effect of posture to the drug administration and/or imaging phase of the experiment: supine methacholine administration followed by supine imaging, prone methacholine administration followed by supine imaging, and prone methacholine administration followed by prone imaging. The two conditions in which imaging was performed supine had similar spatial patterns of bronchoconstriction despite a change in posture during methacholine administration; the odds ratio for recurrent constriction was mean (SD) = 7.4 (3.9). Conversely, dissimilar spatial patterns of bronchoconstriction emerged when posture during imaging was changed; the odds ratio for recurrent constriction between the prone methacholine/supine imaging condition and the prone methacholine/prone imaging condition was 1.2 (0.9). Logistic regression showed that height above the dependent lung border was a significant negative predictor of constriction in the two supine imaging conditions ($P < 0.001$ for each) but not in the prone imaging condition ($P = 0.20$). These results show that the spatial pattern of methacholine bronchoconstriction is recurrent in the supine posture, regardless of whether methacholine is given prone or supine but that prone posture during imaging eliminates that recurrent pattern and reduces its dependence on gravitational height.

NEW & NOTEWORTHY The spatial pattern of methacholine bronchoconstriction in the supine posture is recurrent and skewed toward the dependent lung, regardless of whether inhaled methacholine is administered while supine or while prone. However, both the recurrent pattern and the gravitational skew are eliminated if imaging is performed prone. These results suggest that gravitational influence on regional lung inflation and airway topography at the time of measurement play a role in determining regional bronchoconstriction in the healthy lung.

bronchoconstriction; methacholine; posture; specific ventilation

INTRODUCTION

Asthmatic bronchoconstriction is spatially heterogeneous (7, 12, 17, 29, 31). During a bronchoconstriction event, self-organized patches of very low ventilation form in some regions of the lung, whereas other regions continue to ventilate normally. The degree to which a patient's specific patchy pattern of low specific ventilation recurs between asthmatic episodes is a question of potential clinical importance.

In general, areas of slow space that recur over time can be understood as manifestations of local anatomical and/or functional properties of the lung. Modeling studies have shown that airway asymmetry can lead to spatially persistent foci of constriction and also that less inflated lung regions are more likely to constrict (21, 31, 32). At least one empirical study (10) has confirmed that less inflated lung regions are more likely to become ventilation defects than are more inflated regions.

In our previous work (8), we showed that many patches of ventilatory slow space resulting from methacholine inhalation recurred at the same spatial location in supine healthy subjects. There was a 46% (odds ratio 7.7) likelihood of bronchoconstricted regions recurring a week later and a 56% (odds ratio 7.7) likelihood of regions recurring 3 mo later. On average, 68% of regions that constricted in the first 2 challenges did so again in the third (odds ratio 9.8). Both recurrent and intermittent regions of bronchoconstriction were more likely to occur in the dependent lung than in the nondependent lung when supine; the volume fraction that constricted was 0.43 in the dependent lung versus 0.10 in the nondependent lung.

The relevance of the second finding (that the dependent lung was more likely to constrict than was the nondependent lung) was limited in our previous work because all elements of the experiment (methacholine administration and imaging) were performed supine. Thus, it was unclear whether the recurrent bronchoconstriction in the dependent lung was due to a gravitationally driven physiological effect or a fixed anatomical effect. In other words, we could not specify whether the data showed a predisposition in the dependent lung or a predisposition in the posterior lung, as these designations refer to the same region when supine. The goal of this study was to discern between these two alternatives by repeating the same experiment in the same subjects in two additional conditions: once with methacholine administered in the prone posture but imaging still performed in the supine posture and once with both

Address for reprint requests and other correspondence: E. Geier, Univ. of California, San Diego, Dept. of Medicine, 9500 Gilman Dr., La Jolla, CA 92093 (e-mail: egeier@ucsd.edu).

Table 1. *Subject characteristics and methacholine dosages used*

Subject	Sex	Age, yr	Height, m	Weight, kg	Seated FEV_1, liters (% predicted)	Methacholine PC_{20}, mg/ml	Methacholine dose, mg/ml
S1	M	21	1.60	59	3.82 (100)	2.8	4
S2	F	27	1.57	45	3.05 (101)	6.3	8
S3	M	27	1.88	96	5.59 (110)	10.0	16
S4	F	28	1.70	77	3.54 (101)	5.2	8
S5	M	41	1.78	83	3.87 (92)	10.9	16
S6	F	27	1.64	66	3.25 (99)	3.3	4
Means ± SD		29 ± 7	1.70 ± 0.12	71 ± 18	3.85 ± 0.91 (101 ± 6)	6.4 ± 3.4	9 ± 5

Three female and three male subjects were re-recruited from our previous study (8). Average age, height, and weight of the subjects are shown in the table as they were reported in the previous study (8). Average FEV_1, measured in the seated position, was 101 ± 6% predicted. Methacholine PC_{20} was determined through the standardized stepwise challenge (22), with the exception it was performed in the supine posture, as reported in the previous study (8). Each subject's methacholine dose was chosen to be the last in the stepwise challenge, i.e., the smallest that elicited a >20% drop in FEV_1. F, female; FEV_1, forced expiratory volume in one second; M, male; PC_{20}, concentration of methacholine that elicits 20% drop in FEV_1, determined by interpolation from an empirically determined dose-response curve.

methacholine administration and imaging performed in the prone posture. These data were then compared with the first set of results from the previously published data set (8), in which both methacholine administration and imaging were performed in the supine posture to look for a systematic difference in the corresponding spatial patterns of bronchoconstriction.

These two additional postural configurations (prone methacholine/supine imaging and prone methacholine/prone imaging) allowed us to address an additional question: if gravity skews the spatial pattern of methacholine constriction, is it gravity at the time of constriction or gravity at the time of imaging (or both) that matters? Skew introduced by gravitational orientation during drug inhalation would be expected to manifest similarly in the data sets in which posture during drug administration was the same (prone methacholine/supine imaging and prone methacholine/prone imaging) whereas skew introduced during imaging would be expected to manifest similarly in the conditions in which posture during imaging was the same (supine methacholine/supine imaging and prone methacholine/supine imaging). If the spatial pattern of constriction is determined primarily at the time of methacholine inhalation, we can infer that it is largely influenced by the pattern of methacholine deposition and that it is relatively static with time. On the other hand, if it is determined during imaging we may infer the opposite: that the spatial pattern of bronchoconstriction is due to factors other than methacholine deposition and that it can change to conform to a new gravitational condition.

METHODS

Human Subjects

The University of California, San Diego Human Research Protection Program reviewed and approved this study. Six subjects, the same from Geier et al. 2018 (8), were re-recruited, each passed a standard MRI safety screen, and all subjects denied any history of cardiopulmonary disease. Each subject provided written, informed consent to participate in the study. Forced expiratory volume in one second (FEV_1) measurements were made using an Easyone diagnostic Spirometer (ndd Medical Technologies, Inc., Andover, MA), and percent predicted values were obtained by comparison to National Health and Nutrition Examination Survey III reference values (9). Subjects had baseline FEV_1 values of 101% (6%). Two additional imaging sessions (prone methacholine/supine imaging and prone methacholine/prone imaging) were acquired; the subjects' concentration of methacholine that elicits 20% drop in FEV_1 (PC_{20}) values [6.4 mg/ml (SD 3.4)], methacholine doses [9 mg/ml (SD 5)] and imaging data from the supine baseline and first methacholine challenge (supine methacholine/supine imaging) from the previously published study were reused (8). Subject data as they were acquired for the previous study (8) are shown in Table 1. The time between study sessions, for each subject, is shown in Table 2. Although all subjects completed all sessions of the study, a technical issue discovered in postprocessing necessitated that the prone baseline and prone methacholine/prone imaging data for two subjects (S2 & S4) be excluded from the analysis (see *Experimental setup* below).

Table 2. *PC_{20} dose determination*

	Days from Study Enrollment for Each Study Session			
	Previous study		Current study	
	PC_{20} dose determination†	Supine baseline and supine Mch/supine imaging†	Prone Mch/supine imaging	Prone baseline and prone Mch/prone imaging
S1	0	86	442	536
S2	0	191	450	—
S3	0	327	567	571
S4	0	86	481	—
S5	0	1	312	319
S6	0	1	145	223
Mean ± SD	0 ± 0	115 ± 225	400 ± 149	464 ± 154

PC_{20} dose determination was performed for each subject on the day in which he or she was enrolled in the study. Time intervals, in days, between enrollment and each subsequent study session for each subject are shown. Only four of our six subjects had valid data for the last study, prone methacholine/prone imaging, because of an error in data acquisition (see METHODS). FEV_1, forced expiratory volume in one second; Mch, methacholine; PC_{20}, concentration of methacholine that elicits 20% drop in FEV_1. †Data from our previously published study (8). —Indicate the two sessions for which data had to be discarded following the discovery of a technical issue in data collection.

Methacholine Bronchoconstriction

In our previous study (8), each subject underwent a standard methacholine challenge test to determine the appropriate concentration of drug that could be used to elicit a moderate bronchoconstriction in the subsequent imaging sessions. Methacholine challenge testing was performed according to the standard procedures established by the American Thoracic Society (24) with the sole modification that the subject was supine during all parts of the challenge. Provocholine (methacholine chloride USP, Methapharm, Inc., Brantford, Canada) was nebulized and administered via a Koko Dosimeter (nSpire Health, Inc., Longmont, CO) in a stepwise fashion, starting at 0.03125 mg/ml and doubling each step until a 20% drop in FEV_1 was achieved. In these subjects, the maximum PC_{20} dose was 16 mg/ml.

For each subject, the methacholine concentration chosen for the rest of the study (Table 1) was the final concentration administered in the stepwise challenge, i.e., the lowest that elicited PC_{20}. Methacholine was administered via a Koko Dosimeter before imaging in either the prone or supine posture, depending on the specific imaging session (Table 2).

Methacholine action peaks between 1 and 4 min after inhalation, reaches a steady state that lasts for an average of 75 min, and then fades for an average of 57 min (5). In all three visits, the specific ventilation (SV) imaging (SVI) protocol took place 15–35 min after methacholine administration in the steady-state period of methacholine action so that SV was as constant as possible during the 20-min acquisition. Methacholine was administered to all subjects in all sessions by the same individual. Each subject was given the same instructions so that breathing during drug inhalation was as standardized as possible between subjects.

Imaging Sessions

MR imaging was performed twice at baseline, once while supine and once while prone, and three times following bronchoconstriction by methacholine. The subjects' posture was modified during methacholine administration and imaging as part of the experiment. The postural conditions were *1*) supine methacholine and supine imaging, *2*) prone methacholine and supine imaging, and *3*) prone methacholine and prone imaging. In the second condition, the subjects were turned from prone to supine directly before imaging, ~10 min after methacholine inhalation. The delay between administration and repositioning was included to ensure that the subjects had reached, while prone and before repositioning, the steady state phase of methacholine action (5). The data for supine baseline and supine methacholine/supine imaging condition were acquired in a previous study (8). The supine methacholine/supine imaging condition is the same as that from the first constriction (*day 1*) in that previous study.

FEV_1 measurements were made before imaging for the baseline scans and between methacholine inhalation (~2 min postadministration) and imaging for the bronchoconstricted scans. Supine baseline imaging was performed the same day as *condition 1*, and prone baseline imaging was performed the same day as *condition 3*. Imaging sessions were always performed in order of 1–3. The time intervals between study sessions are shown in Table 2. The long duration of the study reflects the fact that subjects were re-recruited from the prior study, and *day 1* of the previous study was treated as *day 1* of the current study.

SVI

SVI is described in detail in Sá et al. (27). This implementation of SVI was the same as in our previous work (8), with the sole exception that the subjects' posture during methacholine delivery and MR imaging was modified. A brief description of SVI is presented here.

Experimental setup. Methacholine was administered while the subject lay prone or supine (depending on the session) via a Koko Dosimeter (nSpire Health, Inc., Longmont, CO) and spirometry was performed to measure FEV_1. The subject was then fitted with a facemask (7600 Series Oro-nasal mask, Hans Rudolph). After a 10-min wait to ensure that methacholine had reached a steady-state plateau, the subject was placed into the scanner (for the condition in which subjects were imaged supine but given methacholine prone, the subjects were reoriented from prone to supine at this point). A flow-bypass device (6) was attached to the subject's facemask and medical oxygen, driven from a tank via 1/4-in. tubing, was supplied to the flow-bypass at a flow rate of ~120 l/min (chosen to exceed maximal inspiratory flow rate). Oxygen was switched on and off through actuation of a three-way valve, which occurred during subject expiration to produce a stepwise change in fraction of inspired oxygen between subsequent inspirations.

Abrupt switches in fraction of inspired oxygen, facilitated by the system above, cause a rise or fall in alveolar oxygen content. Oxygen diffuses rapidly into the tissue, and the concentration of oxygen dissolved in tissue manifests as a change in T_1-weighted signal. The rate of change from one steady state of oxygenation (and thus MR signal) to another is directly related to the rate at which resident alveolar gas is being replenished by inhaled gas. Expressed as a ratio of volumes, this is the volume of inspired gas that reaches the voxel during inspiration divided by its previous end expiratory volume ($\Delta V/V_o$) and is termed SV. Thus, SV was determined by T_1 imaging while subjects alternately breathed room air and 100% oxygen over 20 min.

The prone imaging data for two subjects (S2 & S4) had to be excluded from our analysis. These subjects laid with their arms over their heads, which obstructed the flow of gas away from the flow bypass system at the mouth. This meant that the subjects rebreathed a mixture of 100% oxygen and room air during the "room air" blocks. Because the precise mixture of gas they were breathing could not be estimated, the signal response for those imaging series could not be modeled.

Image acquisition. Using a 1.5T EXCITE HDx TwinSpeed MRI system (General Electric Medical Systems, Milwaukee, WI) and an eight-element torso coil, four two-dimensional, abutting 15-mm-thick sagittal slices of the right lung were acquired with a single-shot fast spin echo after a global inversion pulse. Inversion recovery times for each slice, respectively (medial to lateral), were 1,100, 1,335, 1,570, and 1,805 ms. Each image slice had a 40 cm $\times$ 40 cm field of view, was acquired at 128 $\times$ 128 resolution, and was reconstructed by the scanner onto a 256 $\times$ 256 matrix.

Image processing. Image processing was performed with custom-written Matlab (Mathworks, Natick, MA) code. Each scan was treated independently, and comparisons between conditions were performed after processing.

For each sagittal slice imaged (4 from each scan) a 220-image time series was created. A generalized dual-bootstrap iterative closest point algorithm (34), used in affine transformation mode, was applied to register images to a selected reference image. Images with a >10% change in imaged lung volume because of transformation were removed from the time series and treated as missing data, based on previous work that has shown that deformations up to 10% volume change can be accurately registered using an affine transformation (1).

Intensity time series were created for voxels within a manually drawn region of interest, and each voxel's time course was correlated with 50 modeled time courses for SV values equally spaced in $\log_{10}$ from 0.01 to 10. The modeled time course that shared the maximum correlation coefficient with the measured time course was selected as the voxel's SV. The spatial map of all voxel SV values was smoothed using a geometric algorithm with a kernel size of 7 voxels (~1 cm^2). Maps from the four sagittal slices in each scan were combined to create a histogram of voxel-SV values for the entire imaged right lung (Fig. 1).

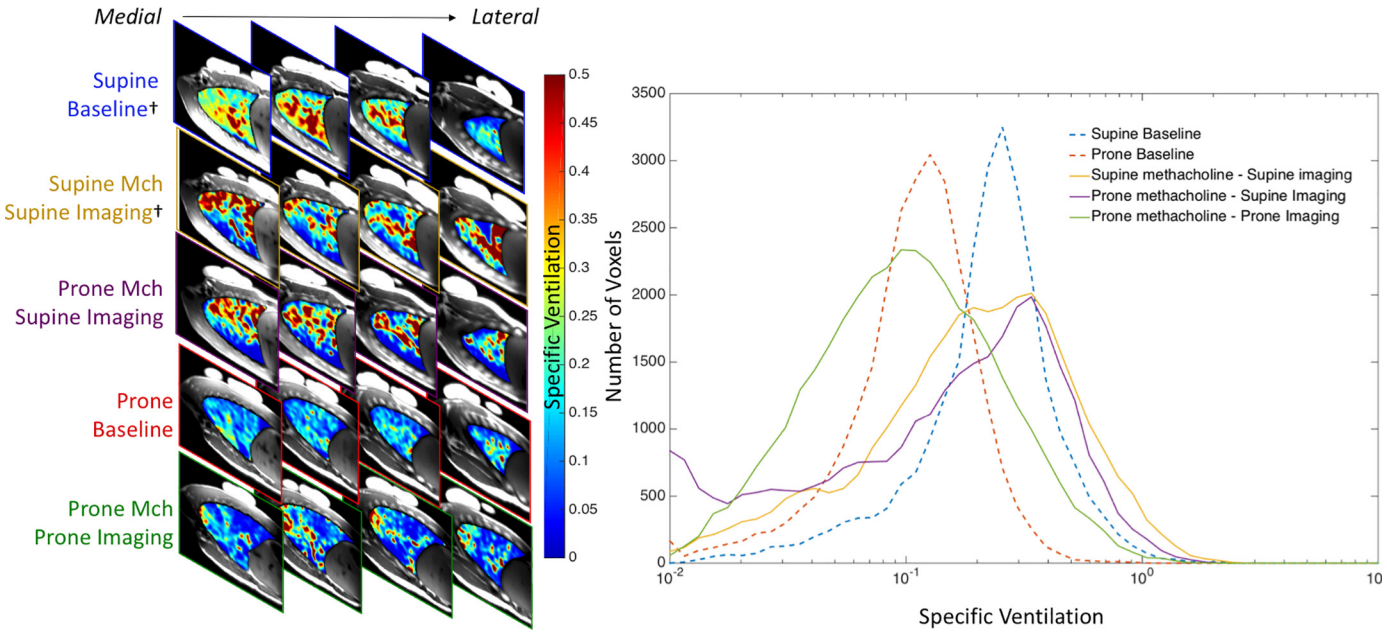

Fig. 1. *Left*: multislice SV maps for one subject (S3) from five imaging sessions. Each row of images represents a separate scanning session/condition. Slices are presented medial to lateral from left to right, with each column representing a sagittal slice of the subject's right lung in each of the sessions. Each map is oriented so that the gravitationally dependent lung is toward the bottom of the imaging frame. In the supine images the posterior lung is gravitationally dependent, whereas in the prone images the anterior lung is gravitationally dependent. *Right*: SV histograms from the same subject (S3) for both baseline (supine and prone) and all three constricted conditions. Baseline data are shown as dashed lines whereas constricted data are shown as solid lines. All histograms are constructed from a compilation of all four imaging slices for the respective condition. †Data from our previously published study (8). Mch, methacholine; SV, specific ventilation.

SV Heterogeneity

SV heterogeneity, as has been reported by our group previously (26), was taken as the full-width at half maximum of a log(Gaussian) function fit to the SV histogram of the entire imaged right lung (Fig. 1). This metric was computed for the two baseline scans and three bronchoconstricted scans for each subject.

Identification of bronchoconstricted regions. SV maps were normalized between conditions to account for changes in global SV, which can be the result of changes in tidal volume and/or FRC. Table 3 shows the prenormalized mean SV and imaged thoracic cage volumes for each condition.

Following normalization, bronchoconstricted maps were spatially correlated with their respective baseline maps, prone to prone and supine to supine. Because the average imaged lung volume during bronchoconstriction was 17% (SD 13) larger than at baseline, a difference that exceeded the 10% limit to which we can confidently register using an affine transformation, we could not use our standard image registration approach. Instead, we divided each multislice set of images into 12 (dependent-nondependent) × 12 (apical-basal) × 4 (medial-lateral, defined by slice) volume elements, the extent of which were based on the size of the lung, redefined for each condition. Comparisons were then made between volume elements in different conditions with the same 12 × 12 × 4 coordinate (Fig. 2). Each of the 12 × 12 × 4 volume elements contained typically between 25 and 100 voxels (depending on its location in the lung). Individual voxels were not compared between conditions.

For the purposes of this study, a volume element i was considered constricted if

$$SV^{i}_{challenge} < 0.5 * SV^{i}_{baseline} \quad \text{and} \quad SV^{i}_{challenge} < \overline{SV}_{baseline} \qquad (1)$$

where $\overline{SV}$ represented the center of the SV distribution.

This imposed two conditions for the constriction designation: *1*) SV must have decreased significantly from baseline and *2*) that a volume element labeled "constricted" was ventilating less than average. These criteria were designed to prevent two types of lung regions from being misclassified as constricted, *1*) regions with consistently low ventilation (even at baseline) that were not necessarily responding to methacholine and *2*) regions with unusually high SV at baseline that may have experienced a reduction in ventilation because of methacholine but not one severe enough to hamper gas exchange.

The constriction designation we use in this study is somewhat analogous to the ventilation defect designation that appears in other, similar studies (10–12, 21, 32, 33). Ventilation defects are clusters of voxels that represent ventilatory slow space. They can be identified through at least three different methods: manually by an experienced observer, through hierarchical k-means clustering (18), or by spatial fuzzy c-means clustering (15).The lung elements in our study that are designated as constricted certainly include voxels that would be designated as ventilation defect, but they also include others that strongly respond to methacholine, as indicated by their >50% drop in FEV_1 but not to the point that they would be considered "defects." For example, a lung element with a relatively high SV (say of 0.3 compared with a lungwide mean SV of 0.2) that fell to an SV of 0.14 (compared with a lungwide mean SV of 0.2) would be considered constricted but would probably not be considered to be part of a defect. Conversely, an element with extremely low SV (say 0.02 compared with a lung-wide mean of 0.2) at baseline that stayed the same after methacholine may be considered a defect in both conditions but would not be classified as constricted in our analysis.

Height from the dependent lung as a predictor of constriction. The vertical height of each 12 × 12 × 4 volume element from the dependent lung border was measured and, along with constriction outcome for each condition, concatenated for all subjects. For each postural condition, a logistic regression model was used to estimate the how the ln(odds) of constriction (our binary outcome variable) varied as a function of a volume element's height (Fig. 3).

Odds ratio for repeat constriction. Constriction maps were compared between days to determine the odds ratio for repeat constriction

Table 3. *Global metrics of constriction for all six subjects in all imaging conditions*

	FEV_1, l/s (% Change From Baseline)				
	Supine baseline†	Prone baseline	Supine Mch/supine imaging†	Prone Mch/supine imaging	Prone Mch/prone imaging
S1	3.55	3.80	2.86 (−19)	2.94 (−23)	3.40 (−11)
S2	2.91		2.53 (−13)	2.49 (−19)	
S3	4.99	5.01	3.92 (−21)	4.11 (−18)	4.10 (−18)
S4	3.05		2.34 (−22)	2.84 (−16)	
S5	3.70	3.56	3.14 (−15)	2.99 (−19)	2.54 (−29)
S6	3.11	2.95	2.38 (−22)	2.06 (−30)	2.59 (−12)
Mean ± SD	3.53 ± 0.78	3.83 ± 0.86	2.86 ± 0.60 (−19 ± 4)	2.91 ± 0.69 (−20 ± 6)	3.16 ± 0.74 (−17 ± 8)
	Mean Specific Ventilation, Prenormalization (% Change from Baseline)				
S1	0.25	0.10	0.10 (−61)	0.19 (−24)	0.12 (26)
S2	0.17		0.09 (−46)	0.08 (−53)	
S3	0.26	0.13	0.28 (5)	0.23 (−12)	0.15 (16)
S4	0.16		0.13 (−16)	0.20 (23)	
S5	0.33	0.24	0.33 (−2)	0.31 (−6)	0.14 (−43)
S6	0.37	0.13	0.21 (−42)	0.15 (−60)	0.16 (22)
Mean ± SD	0.26 ± 0.08	0.15 ± 0.07	0.19 ± 0.10 (−27 ± 27)	0.19 ± 0.08 (−22 ± 31)	0.14 ± 0.01 (5 ± 32)
	Imaged Thoracic Cage Volume, ml (% Change from Baseline)				
S1	851	844	927 (9)	831 (−2)	811 (−4)
S2	600		732 (22)	655 (9)	
S3	930	980	1,206 (30)	1,141 (23)	1,371 (40)
S4	559		785 (40)	698 (25)	
S5	509	736	518 (2)	556 (9)	827 (12)
S6	497	551	561 (13)	567 (14)	637 (16)
Mean ± SD	658 ± 186	778 ± 181	788 ± 254 (19 ± 14)	741 ± 220 (13 ± 10)	912 ± 318 (16 ± 18)
	FWHM of SV Distribution (% Change from Baseline)				
S1	0.44	0.47	0.92 (110)	0.79 (80)	0.43 (−9)
S2	0.32		1.03 (224)	0.79 (343)	
S3	0.43	0.48	0.91 (111)	0.99 (129)	0.93 (93)
S4	0.57		0.46 (−20)	0.49 (−15)	
S5	0.61	0.52	0.55 (−9)	1.12 (85)	0.92 (78)
S6	0.32	0.52	1.00 (210)	1.86 (475)	0.94 (80)
Mean ± SD	0.45 ± 0.12	0.50 ± 0.02	0.81 ± 0.25 (104 ± 104)	1.11 ± 0.48 (183 ± 186)	0.80 ± 0.25 (60 ± 47)
	Volume Fraction of Lung Constricted				
S1			0.32	0.27	0.06
S2			0.25	0.32	
S3			0.38	0.34	0.39
S4			0.34	0.20	
S5			0.19	0.19	0.29
S6			0.27	0.30	0.31
Mean ± SD			0.29 ± 0.07	0.27 ± 0.06	0.26 ± 0.14

The two left columns show the baseline (premethacholine) values of each metric measured in both the supine and prone postures. See text for details. Postmethacholine values are shown in the right three sets of columns with headings referring to their respective conditions. Relative changes from baseline are indicated as percentages. Only four of our six subjects had valid data for the last study, prone methacholine/prone imaging, because of an error in data acquisition (see METHODS). FEV_1, forced expiratory volume in one second; FWHM, full width half maximum; Mch, methacholine; SV, specific ventilation. †Indicates data from our previously published study (8).

of a 12 × 12 × 4 volume element in the second or third (prone methacholine/supine imaging or prone methacholine/prone imaging, respectively) conditions given a constriction in the first (supine methacholine/supine imaging) condition, and the odds ratio for repeat constriction in the third (prone methacholine/prone imaging) given a constriction in the second (prone methacholine/supine imaging). For the comparison between supine methacholine/supine imaging and prone methacholine/supine imaging, this process was straightforward because the imaging planes were in the same position and orientation. The comparisons between the supine imaging conditions, supine methacholine/supine imaging and prone methacholine/supine imaging, and the prone methacholine/prone imaging condition is less intuitive because of the flip in gravitational orientation. A volume element in the dependent lung while supine is now in the nondependent lung while prone, and vice versa. Because of the differences in lung container shape and gravitational stretch between the prone and supine postures, it is likely that each volume element encompasses a slightly different region of lung tissue after the flip (e.g., a basal/posterior unit was dependent and compressed while supine, but is now nondependent and stretched while prone, so it may now contain less tissue and/or some tissue from elements that were neighbors while supine). Thus, comparisons between the supine methacholine/supine imaging and prone methacholine/prone imaging conditions must be made with this limitation in mind.

Statistics

R (25) was used for all statistical analyses performed in this study. Paired *t*-tests were performed using the stats package (25) to determine how prone versus supine posture affected baseline measurements of FEV_1, SV heterogeneity, mean SV, and thoracic cage volume. Only data from subjects with both measurements were used for this last computation.

Linear mixed effects models were generated using the lme4 package (2) to investigate the dependence of metrics of constriction (Table 2, Fig. 4) on the postural condition of the experiment, given the missing measurements for two subjects. For each model, the postural condition of the experiment (supine methacholine/supine imaging, prone methacholine, supine imaging, etc.) or pair of experiments was taken as a fixed effect and subject was taken as a random effect. *P*

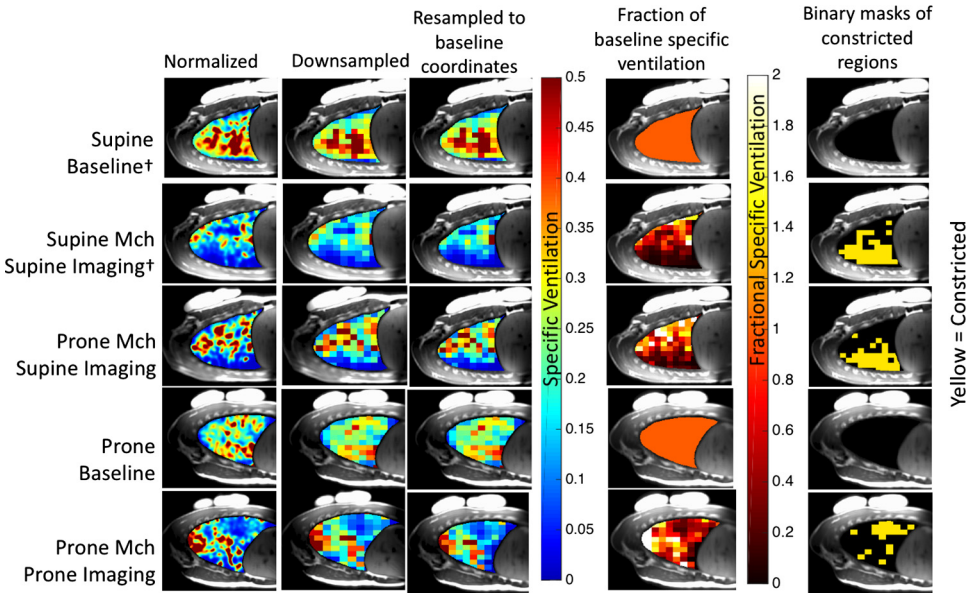

Fig. 2. Processing flow for subject S3's midclavicular (second slice) SV map in all five study conditions. The first column of each row shows the normalization based on the total SV (compiled from all four slices, only the midclavicular slice is shown) of the supine baseline condition. Maps from each slice were then downsampled (second column) to a 12 × 12 grid of volume elements and then projected onto the relevant baseline image (third column) for further analysis. Fractional SV (fourth column) was computed by dividing maps by the relevant baseline condition map. For baseline data this metric is, by definition, 1.0 everywhere. Elements were classified as constricted (fifth column) if their fractional SV was less than 0.5 and their normalized SV was less than the center of the baseline SV distribution. In each case, the gravitationally dependent lung is shown at the bottom of the image, as it was during imaging. †Data from our previously published study (8). Mch, methacholine; SV, specific ventilation.

values were obtained by a likelihood ratio test of the model with the fixed effect (postural condition) versus a null model with no fixed effect.

Logistic regression models were fit using the glm package (25) to characterize how the likelihood of constriction varied as a function of height above the dependent lung. McFadden's pseudo-R^2 was used to estimate the strength of the model fit (22). Formally, McFadden's $R^2 = 1 - \ln(L_M)/\ln(L_0)$ where L_M is the likelihood for the model with the chosen predictors and L_0 is the likelihood for a null model with no predictors. A higher value of McFadden's R^2 means that more of the variance in the data is being explained by the logistic regression model (14). The P value (Wald Test) for each model and the fit coefficient for height are also reported in Fig. 3. To characterize the uncertainty of our logistic regression models, we used a data-driven bootstrapping approach. For each postural condition, we resampled with replacement from our measured data set of height versus constriction (keeping the links between the two intact) until a set of equal size to the original was obtained. A logistic regression was then fit to this resampled data set, and the P value, fit coefficients, and McFadden's R^2 of the model were recorded. We repeated this process 1,000 times and took the standard deviation of each set of 1,000 outputs to be the uncertainty of our original fit.

A log transformation was applied to the odds ratios account for their intrinsic positive skew and thus make statistical testing possible

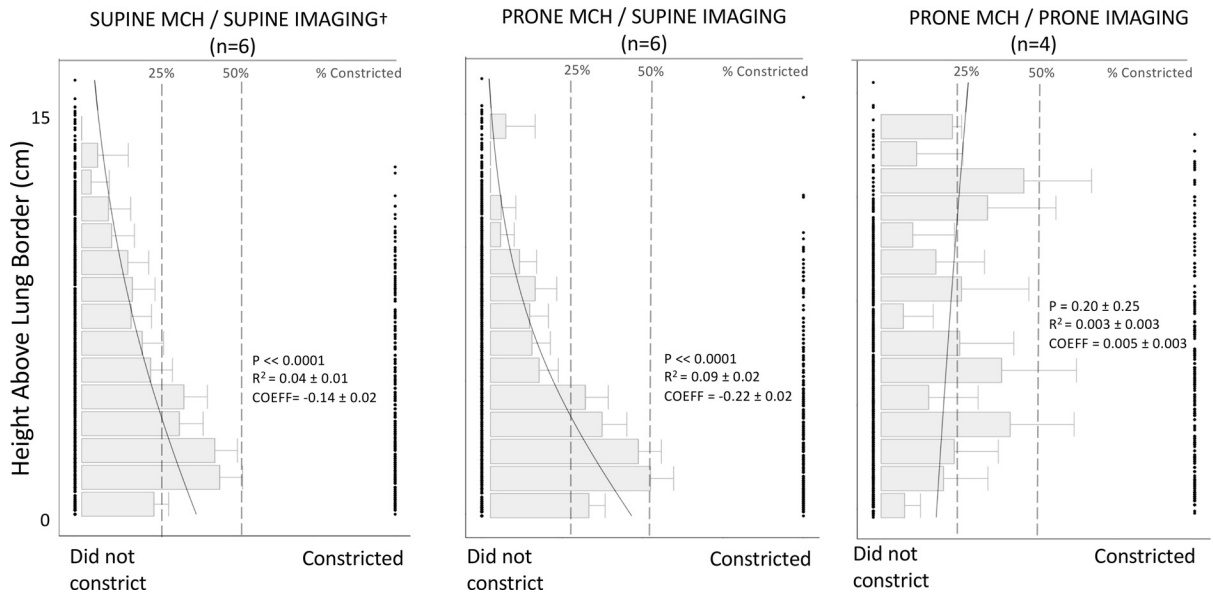

Fig. 3. For supine Mch/supine imaging (*left*), prone Mch/supine imaging (*middle*), and prone Mch/prone imaging (*right*), the constricted/nonconstricted binary outcome variable is shown as a function of height above the dependent lung border for each volume element in the study (each element is a point). A black solid line depicts the average best-fit logistic regression model, as detailed in the text. Average and standard deviations for the bootstrapped P values, McFadden's pseudo-R^2s, and fit coefficients (COEFF) are indicated next to the fit line. Also depicted as semishaded horizontal bars in each graph are the proportions of volume elements in each 1-cm bin that constricted following Mch, with error bars indicating the upper bound of the 95% confidence interval for each. The number (n) of subjects whose data was used to construct each logistic regression is indicated above each chart. †Data from our previously published study (8). Mch, methacholine.

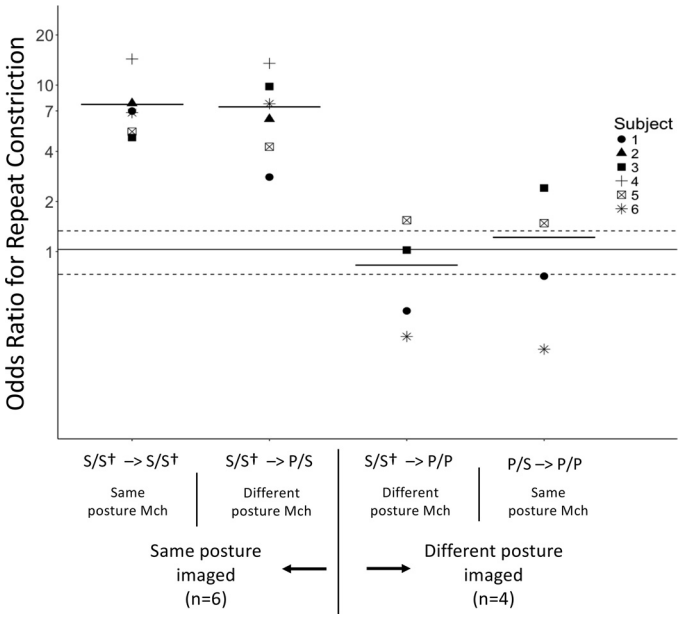

Fig. 4. Scatterplot of the odds ratios, on a log scale, for repeat constriction given a prior constriction in a previous study. The postures for each phase of the two studies in each pair are indicated on the *x*-axis; supine (S) and prone (P) for methacholine/imaging respectively, e.g., S/S refers to supine methacholine/supine imaging and S/S → P/S refers to the comparison between the supine methacholine supine imaging condition and the prone methacholine/supine imaging condition. Intrapair differences in posture during methacholine and/or imaging are indicated below the *x*-axis. A linear mixed effects model showed a significant fixed effect of experiment pair ($P < 0.001$) on the odds ratio for repeat constriction. Subjects are given unique symbols, and short solid lines represent group averages for each pair of studies. The solid horizontal line spanning the plot at 0.023 represents the mean log(odds) for 1,000 bootstrap samples with spatially random constriction, and the dashed lines represent two standard deviations of the bootstrapped means in each direction. Previous constriction was predictive of subsequent constriction for the leftmost two pairs [ln(odds) of data was greater than ln(odds) of spatially random model, $P = 0.004$ for S/S → S/S and $P = 0.006$ for S/S → P/S (Bonferroni-corrected)] but not for the rightmost two pairs [ln(odds) of data was not greater than ln(odds) of spatially random model, $P > 0.99$ for S/S → P/P and $P > 0.99$ for P/S → P/P (Bonferroni-corrected)]. The number (*n*) of subjects whose data was used in each comparison is indicated below the *x*-axis. †Data from our previously published study (8).

(3, 4). To help interpret the odds ratios for repeat constriction, we modeled the null hypothesis that constriction in the first condition does not predict constriction in a subsequent condition. To do this, we computed the odds ratio for repeat constriction between the first condition, supine methacholine/supine imaging, and 1,000 modeled data sets in which all subjects had randomly allocated (but proportionally representative, as defined by each subject's average fraction of constricted lung between the subsequent two conditions) constriction. The average of these 1,000 modeled study pairs was taken to represent the odds ratio for repeat constriction, assuming no spatial specificity for constriction in the second condition. A bootstrap randomization test with 1,000 iterations was used to determine if the observed ln(odds) for repeat constriction were statistically different from the null model for each pair of studies. Because four comparisons were performed (one for each pair of studies), the *P* values from these bootstrap tests were Bonferroni-corrected.

Similarly, we modeled a first-order hypothesis that constriction is predicted only by the effect of height above the dependent lung border as characterized by our best-fit logistic regression models (Fig. 3). For this, 1,000 modeled data sets for each postural condition were computed in which each lung element's likelihood of constriction was determined by its height above the dependent lung. The odds ratio for constriction in the model data, given constriction in the observed data, was then computed for each of the 1,000 repeats for each comparison of interest. The mean and standard deviation of these 1,000 odds ratios were taken to be representative of the odds ratio for repeat constriction within/between postural conditions, given the predisposing factor of height above the dependent lung alone.

Throughout the text, results are presented as mean (standard deviation).

RESULTS

Baseline Measurements

At baseline neither FEV_1, nor the full width half maximum of the SV distribution, nor the thoracic cage volume varied between the prone and supine postures ($P = 0.89$, $P = 0.47$, and $P = 0.21$, respectively, two-tailed paired *t*-tests). Mean SV at baseline was lower while prone than while supine ($P = 0.02$).

Lung-Wide Metrics of Constriction

FEV_1 decreased for all subjects following methacholine (as imposed by the study design), and the heterogeneity of SV increased on average (Table 3). Linear mixed effects models showed that posture during methacholine inhalation and/or imaging had no significant fixed effect on the methacholine-induced fall in FEV1 ($P = 0.96$) and no significant fixed effect on the increase in SV heterogeneity as measured by the change in the full width half maximum of the subjects' SV distributions ($P = 0.09$). The percent change in mean SV did not differ significantly based on the subjects' posture during methacholine delivery and/or imaging ($P = 0.18$), nor did the change in thoracic cage volume ($P = 0.17$).

On average, 29% (SD 7) of the lung (by volume) constricted following supine methacholine inhalation when the subject was imaged supine, 27% (SD 6) of the lung constricted following prone methacholine inhalation when the subject was imaged supine, and 26% (SD 14) of the lung constricted following prone methacholine inhalation when the subject was imaged prone (Table 3). A linear mixed effects model showed no significant fixed effect of this metric on posture during methacholine and/or imaging ($P = 0.80$).

Height from the Dependent Lung Border as a Predictor of Constriction

Figure 3 shows the binary outcome variable, constriction/nonconstriction, as a function of height above the dependent lung border, along with the corresponding best fit logistic regression model. Bar graphs of the fraction of lung that constricted in each 1-cm bin of height are superimposed. A volume element's height from the dependent lung border was a significant predictor of constriction in the two conditions in which imaging was performed supine (supine methacholine/supine imaging and prone methacholine/prone imaging) but not when imaging was performed prone (prone methacholine/prone imaging). The coefficient of the logistic regression was larger (more negative), and the predictive value of height (measured by McFadden's pseudo-R^2) was stronger in the prone methacholine/supine imaging condition than in the supine methacholine/supine imaging condition. The coefficient of a logistic regression, which is somewhat analogous to the slope of a linear regression, quantifies the rate by which the

ln(odds) of an outcome (in this case, constriction vs. nonconstriction) changes as a function of the independent variable (in this case, height above the dependent lung).

Odds Ratio for Recurrent Constriction of a Volume Element

In our previously published study (8) we showed that a lung volume element that had previously constricted was 7.7 times more likely [odds ratio 7.7 (SD 3.5)] to constrict during a subsequent study in which posture was the same both during methacholine inhalation and while imaging. In this study, we computed the odds ratios for repeat constriction between data from the first imaging session of our previously published study, in which supine methacholine administration was followed by supine imaging, and the new data acquired during two altered experimental conditions, prone methacholine administration followed by supine imaging, and prone methacholine administration followed by prone imaging (Fig. 4). Furthermore, we computed the odds ratio for repeat constriction between the two new conditions in this study, prone methacholine/supine imaging and prone methacholine/prone imaging, to determine the effect of solely modifying posture during imaging. We found that the odds ratio for repeat constriction between supine methacholine/supine imaging and prone methacholine/supine imaging was 7.4 (SD 3.9), the odds ratio for repeat constriction between the supine methacholine/supine imaging condition and the prone methacholine/prone imaging condition was 0.8 (SD 0.6), and the odds ratio for repeat constriction between the prone methacholine/supine imaging and prone methacholine/prone imaging conditions was 1.2 (SD 0.9) (Fig. 4).

A linear mixed effects model showed that the log-transformed odds ratios for repeat constriction varied between study pairs ($P < 0.001$). One thousand iterations of a model of our experiment with random (but proportionally representative) patterns of constriction showed that completely random constriction in the second condition (for all subjects) would result in an average odds ratio of 1.0 (SD 0.2). For the two study pairs in which the posture during imaging was the same (supine), a previous constriction event in a lung element was a strong predictor for a subsequent constriction event; the ln(odds) of the data was greater than the than ln(odds) of the spatially random model, $P = 0.004$ for supine methacholine/supine imaging $\rightarrow$ supine methacholine/supine imaging and $P = 0.006$ for supine methacholine/supine imaging $\rightarrow$ prone methacholine/supine imaging (Bonferroni-corrected). For the two study pairs in which the posture during imaging was different (prone vs. supine) a previous constriction event in a lung element did not predict a subsequent constriction event; the ln(odds) of the data was not different than the than ln(odds) of the spatially random model, $P > 0.99$ for supine methacholine/supine imaging $\rightarrow$ prone methacholine/prone imaging, and $P > 0.99$ for prone methacholine/supine imaging $\rightarrow$ prone methacholine/prone imaging [Bonferroni-corrected]).

First-order models of constriction, which incorporated the logistic regressions depicted in Fig. 3, allowed us to calculate the expected odds ratio for recurrent constriction given the effect of height above the dependent lung. These models showed that the height dependence alone would result in an odds ratio of 1.3 (SD 0.4) for repeat constriction between two subsequent supine methacholine/supine imaging challenges, an odds ratio of 1.4 (SD 0.5) for repeat constriction between the supine methacholine/supine imaging and prone methacholine/supine imaging condition, and an odds ratio of 1.0 (SD 0.3) for repeat constriction between prone methacholine/supine imaging and prone methacholine/prone imaging condition.

DISCUSSION

In brief, our data lead to two main inferences: *1*) administering methacholine while prone as opposed to while supine neither dampens the nondependent-dependent gradient of constriction nor diminishes the likelihood of a volume element recurrently constricting if imaging is still performed supine, and *2*) the prone posture while imaging eliminates the nondependent-dependent gradient of constriction and greatly diminishes the likelihood of a volume element recurrently constricting when compared with a previous supine imaging session.

Constriction in the supine methacholine/supine imaging study was a strong predictor of constriction in the prone methacholine/supine imaging condition, even though methacholine was administered in a different posture. In contrast, a volume element that constricted in the prone methacholine/supine imaging session has a no better than random chance of constricting in the prone methacholine/prone imaging session [odds ratio 1.2 (SD 0.9) vs. 1.0 (SD 0.2) for the random model, $P > 0.99$]. This suggests that the spatial pattern of methacholine bronchoconstriction is mostly independent of posture during drug inhalation, yet it is profoundly influenced by posture at the time of measurement. Because drug action peaked and reached a plateau in the same posture as methacholine was administered, we can further infer that posture during the peak of methacholine action has little effect on the spatial pattern of methacholine constriction if posture is subsequently changed.

It has been shown that methacholine distributes heterogeneously throughout the lung and that changing posture from seated to supine alters the deposition pattern of the drug (28). Furthermore, it has been shown that heterogeneity of deposition affects the potency of methacholine (20). However, our data make it clear that the pattern of methacholine deposition in the prone versus supine posture does not affect the degree to which regions of lung recurrently constrict, which means that the drug itself or the mechanisms by which it becomes spatially selective must be somehow distributed throughout the lung.

The pattern of methacholine deposition may, however, affect the gravitational pattern of constriction in a paradoxical way. The skew toward constriction in the dependent lung was stronger (larger effect size measured by McFadden's R^2) and steeper (more negative fit coefficient) in the prone methacholine/supine imaging condition than it was in the supine methacholine/supine imaging condition. It is unclear why this would be the case but one explanation may be that more uniform distribution of methacholine in the prone posture causes more uniform smooth muscle activation, which in turn allows for underlying physiological processes to manifest more clearly.

The dependent skew in constriction evident in our two supine imaging conditions has been reported previously in subjects with asthma (10, 11, 19, 30) and may be driven by gravitational influence on regional lung inflation. The dependent lung is compressed by the weight of the lung above it (13) and thus is likely to be less inflated than tissue in the nonde-

pendent lung. One of several predictions made by modeling studies is that the decrease in expansion-mediated parenchymal forces characteristic of less inflated regions leads to easier airway closure and therefore, a predisposition toward constriction under stress (31–33). The skew toward constriction in the dependent lung in our data is consistent with this prediction. The less significant dependent skew in the prone imaging condition may also be consistent with a model of expansion-mediated parenchymal forces predisposing a region toward bronchoconstriction, because studies have shown that lung density is more vertically homogeneous while prone than while supine (13, 23), and at least one study (16) suggests that alveolar stress is more uniform while prone than while supine.

Furthermore, the less significant dependent skew while prone echoes part of a previous report by Harris et al. (11). Utilizing ^{13}NN-saline positron emission tomography, Harris showed that the vertical gradient in lung fractional gas content changed following methacholine in the supine posture but not in the prone posture. Thus, the gravitational effect of methacholine constriction on lung fractional gas content was stronger while supine than while prone, just as the gravitational effect on likelihood of constriction was stronger in our study while supine than while prone. Another finding of the Harris study [that ventilation defects were smaller in the prone posture than in the supine posture (25% vs. 41%)] is visible as a very small effect in our study that was not statistically significant; the volume fraction of constriction in our subjects was less while prone [26% (SD 13)] than while supine [27% (SD 6) for prone methacholine, 29% (SD 7) for supine methacholine]. However, at least one finding of the Harris study (that ventilation defects were, by and large, dependent even while prone) is not evident in our study. The best-fit logistic regression model to the prone methacholine/prone imaging condition did not find a significant nondependent-dependent trend ($P = 0.20$) (Fig. 3). This may be because of the inherent difference in our definition of constriction versus the definition of a ventilation defect (see *Identification of bronchoconstricted regions* above).

However, only part of the overall spatially repeatable pattern of bronchoconstriction can be explained by gravitational height alone. By using first-order models, we predicted that the odds ratio for repeat constriction given the effect of height alone should be 1.3 (SD 0.4) for repeated supine methacholine/supine imaging sessions and 1.4 (SD 0.5) for recurrent constriction between supine methacholine/supine imaging and prone methacholine/supping imaging. These predictions based on gravitational tendency are much less than the observed odds ratios: 7.7 (SD 3.5) for repeat supine methacholine/supine imaging sessions and 7.4 (SD 3.9) for repeat constriction between supine methacholine/supine imaging and prone methacholine/supine imaging, which suggests that one or more additional factors must be at play. Furthermore, the relatively modest effect sizes of the height-based logistic regressions [Fig. 3, McFadden's $R^2 = 0.04$ (SD 0.01) for supine methacholine/supine imaging and McFadden's $R^2 = 0.09$ (SD 0.02) for prone methacholine/supine imaging] make it clear that gravitational height alone cannot account for the markedly recurrent pattern of bronchoconstriction.

In healthy subjects without anatomical remodeling because of disease, gravitational compression of lung tissue may act in concert with other factors to enforce a spatially recurrent pattern of bronchoconstriction. Leary et al. (21) have shown that recurrent constriction can also be caused by the innate asymmetry of the airway tree. Although airway asymmetry alone cannot be responsible for spatially recurrent bronchoconstriction (or else the pattern would have been at least partially recurrent between the supine and prone postures), it may play a significant role in conjunction with gravity. It is likely that innate anatomical features, superimposed upon by gravitational compressive/expansive forces, form a topography that accounts for the predisposition of some regions toward constriction. In subjects with asthma, one might speculate that structural pathology and inflammation could add yet more layers of to the topography.

It is also interesting to note that in Fig. 1, some voxels paradoxically experienced an increase in SV following methacholine or else remained close to their baseline value of SV. Modeling of bronchoconstriction in an airway tree has predicted that ventilation can be redistributed away from ventilation defects to other regions of the lung to maintain adequate overall ventilation (32). In our study, the between-subjects average fractional SV (methacholine SV/baseline SV) in lung units that were not classified as constricted was 1.29 (0.15). This means that there was a relative increase (postnormalization) in SV outside of the constricted regions, which is consistent with the previous model prediction.

Limitations. Our study is limited by the fact that we used a binary definition of constriction that is based on a change between baseline SVI and methacholine SVI. The marked similarity between the group average constriction fraction in each postural condition could hint that a particular percentage of lung will always be classified as constricted because of the method alone. However, there is a large degree of variability in constriction fraction between different days in the same subject (maximum intrasubject variability for this study was 0.06–0.32). Furthermore, the choice to use a PC_{20} dose of methacholine was made to elicit bronchoconstriction that was as consistent as possible between study days and between subjects, so this similarity in group average constricted fraction may be a result of this choice.

Another limitation is that the SVI measurement takes 18 min and 20 s to complete, although the bronchoconstriction in our study is due to a drug with a transient effect. Although methacholine action, on average, plateaus for 75 min after drug administration, the effect is variable between subjects (5). Thus, it is possible that bronchoconstriction ebbed during the SVI measurement because of metabolism of the drug. The SVI technique, as implemented, cannot capture this dynamic effect. Instead, it would report the time-averaged SV for each voxel. To avoid this complication, we imaged 15–35 min after methacholine administration, while drug action was as steady state as possible.

Our study is also limited because of a small sample size, especially for the prone methacholine/prone imaging condition in which data from two subjects had to be excluded. There is potential for sampling bias, especially when making comparisons between conditions. However, in Fig. 4, all four subjects who had acceptable data for each condition saw the same effect of changing posture during imaging—a decrease in the odds ratio for repeat constriction. In Fig. 3, the prone methacholine/prone imaging logistic regression was using data from 4 subjects instead of 6, but still encompassed 1,113 total lung regions. To test for differences between conditions in each of

our metrics, we used a linear mixed-effects model to account for the difference in sample size.

A further limitation of our study is that the imaged volume encompassed only 80% of one lung. The absence of the most medial and most lateral aspects of the right lung in our analysis is unlikely to affect our results, as our previous study showed a lack of difference in the spatial pattern of constriction between the medial and lateral slices (8). However, any systematic differences in the effect of posture on bronchoconstriction in the left versus right lung will not have been captured by this study.

Conclusion

The results of our study suggest that height above the dependent lung is a predictor of bronchoconstriction following methacholine when a subject lies supine but is not a predictor when a subject lies prone. This may suggest that differences in regional lung inflation play a role in determining the spatial pattern of methacholine bronchoconstriction, because lung inflation is more homogeneous while prone than while supine (13, 23). Furthermore, we have shown that changing posture during methacholine administration from supine to prone neither affects the spatial repeatability of constriction nor decreases the dependent (posterior) skew in constriction if imaging is subsequently performed supine. This suggests that the effects of the methacholine deposition pattern on the spatial pattern of bronchoconstriction, if they exist, can be overwhelmed by mechanical and/or anatomical factors.

ACKNOWLEDGMENTS

The authors thank Dr. Laura Crotty-Alexander for acting as medical advisor and Katie Kinninger for help with the methacholine challenge tests. This study relied upon algorithms developed by Amran K. Asadi and Ian Neuhart. Fred Cook developed hardware that made our protocol more streamlined and robust. A. Kizhakke Puliyakote provided help during data collection. We are extremely grateful to our subjects, who were each kind enough to come back for these follow-up studies.

GRANTS

Eric Geier's work was funded by NHLBI F30 HL-127980-3. The work was also funded by NHLBI R01 HL-119263.

DISCLOSURES

No conflicts of interest, financial or otherwise, are declared by the authors.

AUTHOR CONTRIBUTIONS

E.T.G., R.J.T., G.K.P., and R.C.S. conceived and designed research; E.T.G., K.K., and R.C.S. performed experiments; E.T.G., K.K., and R.C.S. analyzed data; E.T.G., K.K., R.J.T., G.K.P., and R.C.S. interpreted results of experiments; E.T.G. and G.K.P. prepared figures; E.T.G. drafted manuscript; E.T.G., K.K., R.J.T., G.K.P., and R.C.S. edited and revised manuscript; E.T.G., K.K., R.J.T., G.K.P., and R.C.S. approved final version of manuscript.

REFERENCES

1. **Arai TJ, Villongco CT, Villongco MT, Hopkins SR, Theilmann RJ.** Affine transformation registers small scale lung deformation. *Conf Proc IEEE Eng Med Biol Soc* 2012: 5298–5301, 2012. doi:10.1109/EMBC.2012.6347190.
2. **Bates D, Mächler M, Bolker B, Walker S.** Fitting linear mixed-effects models using lme4. *J Stat Softw* 67: 1–48, 2015. doi:10.18637/jss.v067.i01.
3. **Bland JM, Altman DG.** Transforming data. *BMJ* 312: 770, 1996. doi:10.1136/bmj.312.7033.770.
4. **Bland JM, Altman DG.** Statistics notes. The odds ratio. *BMJ* 320: 1468, 2000. doi:10.1136/bmj.320.7247.1468.
5. **Cartier A, Malo JL, Bégin P, Sestier M, Martin RR.** Time course of the bronchoconstriction induced by inhaled histamine and methacholine. *J Appl Physiol Respir Environ Exerc Physiol* 54: 821–826, 1983. doi:10.1152/jappl.1983.54.3.821.
6. **Cook FR, Geier ET, Asadi AK, Sá RC, Prisk GK.** Rapid prototyping of inspired gas delivery system for pulmonary MRI research. *3D Print Addit Manuf* 2: 196–203, 2015.
7. **Dunnill MS.** The pathology of asthma, with special reference to changes in the bronchial mucosa. *J Clin Pathol* 13: 27–33, 1960. doi:10.1136/jcp.13.1.27.
8. **Geier ETT, Neuhart I, Theilmann RJJ, Prisk GKK, Sá RCC.** Spatial persistence of reduced specific ventilation following methacholine challenge in the healthy human lung. *J Appl Physiol (1985)* 124: 1222–1232, 2018. doi:10.1152/japplphysiol.01032.2017.
9. **Hankinson JL, Odencrantz JR, Fedan KB.** Spirometric reference values from a sample of the general U.S. population. *Am J Respir Crit Care Med* 159: 179–187, 1999. doi:10.1164/ajrccm.159.1.9712108.
10. **Harris RS, Fujii-Rios H, Winkler T, Musch G, Vidal Melo MF, Venegas JG.** Ventilation defect formation in healthy and asthma subjects is determined by lung inflation. *PLoS One* 7: e53216, 2012. [Erratum in PLoS One 9: 2014.] doi:10.1371/journal.pone.0053216.
11. **Harris RS, Winkler T, Musch G, Vidal Melo MF, Schroeder T, Tgavalekos N, Venegas JG.** The prone position results in smaller ventilation defects during bronchoconstriction in asthma. *J Appl Physiol (1985)* 107: 266–274, 2009. doi:10.1152/japplphysiol.91386.2008.
12. **Harris RS, Winkler T, Tgavalekos N, Musch G, Melo MF, Schroeder T, Chang Y, Venegas JG.** Regional pulmonary perfusion, inflation, and ventilation defects in bronchoconstricted patients with asthma. *Am J Respir Crit Care Med* 174: 245–253, 2006. doi:10.1164/rccm.200510-1634OC.
13. **Hopkins SR, Henderson AC, Levin DL, Yamada K, Arai T, Buxton RB, Prisk GK.** Vertical gradients in regional lung density and perfusion in the supine human lung: the Slinky effect. *J Appl Physiol (1985)* 103: 240–248, 2007. doi:10.1152/japplphysiol.01289.2006.
14. **Hu B, Shao J, Palta M.** Pseudo-R2 in logistic regression model. *Stat Sin* 16: 847–860, 2006.
15. **Hughes PJC, Horn FC, Collier GJ, Biancardi A, Marshall H, Wild JM.** Spatial fuzzy c-means thresholding for semiautomated calculation of percentage lung ventilated volume from hyperpolarized gas and ^{1}H MRI. *J Magn Reson Imaging* 47: 640–646, 2018. doi:10.1002/jmri.25804.
16. **Johnson NJ, Luks AM, Glenny RW.** Gas exchange in the prone posture. *Respir Care* 62: 1097–1110, 2017. doi:10.4187/respcare.05512.
17. **King GG, Eberl S, Salome CM, Meikle SR, Woolcock AJ.** Airway closure measured by a technegas bolus and SPECT. *Am J Respir Crit Care Med* 155: 682–688, 1997. doi:10.1164/ajrccm.155.2.9032213.
18. **Kirby M, Heydarian M, Svenningsen S, Wheatley A, McCormack DG, Etemad-Rezai R, Parraga G.** Hyperpolarized 3He magnetic resonance functional imaging semiautomated segmentation. *Acad Radiol* 19: 141–152, 2012. doi:10.1016/j.acra.2011.10.007.
19. **Kruger SJ, Niles DJ, Dardzinski B, Harman A, Jarjour NN, Ruddy M, Nagle SK, Francois CJ, Sorkness RL, Burton RM, Munoz del Rio A, Fain SB.** Hyperpolarized helium-3 MRI of exercise-induced bronchoconstriction during challenge and therapy. *J Magn Reson Imaging* 39: 1230–1237, 2014. doi:10.1002/jmri.24272.
20. **Laube BL, Norman PS, Adams GK III.** The effect of aerosol distribution on airway responsiveness to inhaled methacholine in patients with asthma. *J Allergy Clin Immunol* 89: 510–518, 1992. doi:10.1016/0091-6749(92)90317-U.
21. **Leary D, Winkler T, Braune A, Maksym GN.** Effects of airway tree asymmetry on the emergence and spatial persistence of ventilation defects. *J Appl Physiol (1985)* 117: 353–362, 2014. doi:10.1152/japplphysiol.00881.2013.
22. **McFadden D.** Conditional logit analysis of qualitative choice behavior, edited by Zarembka P. In: *Frontiers in Econometrics*. New York: Academic, p. 105–142, 1973.
23. **Petersson J, Rohdin M, Sánchez-Crespo A, Nyrén S, Jacobsson H, Larsson SA, Lindahl SGE, Linnarsson D, Neradilek B, Polissar NL, Glenny RW, Mure M.** Posture primarily affects lung tissue distribution with minor effect on blood flow and ventilation. *Respir Physiol Neurobiol* 156: 293–303, 2007. doi:10.1016/j.resp.2006.11.001.
24. **Popa V.** ATS guidelines for methacholine and exercise challenge testing. *Am J Respir Crit Care Med* 163: 292–293, 2001. doi:10.1164/ajrccm.163.1.16310b.
25. **R Development Core Team.** R: a language and environment for statistical computing. Vienna, Austria: R Foundation for Statistical Computing. https://www.r-project.org/, 2016.

26. **Sá RC, Asadi AK, Theilmann RJ, Hopkins SR, Prisk GK, Darquenne C.** Validating the distribution of specific ventilation in healthy humans measured using proton MR imaging. *J Appl Physiol (1985)* 116: 1048–1056, 2014. doi:10.1152/japplphysiol.00982.2013.
27. **Sá RC, Cronin MV, Henderson AC, Holverda S, Theilmann RJ, Arai TJ, Dubowitz DJ, Hopkins SR, Buxton RB, Prisk GK.** Vertical distribution of specific ventilation in normal supine humans measured by oxygen-enhanced proton MRI. *J Appl Physiol (1985)* 109: 1950–1959, 2010. doi:10.1152/japplphysiol.00220.2010.
28. **Sá RC, Zeman KL, Bennett WD, Prisk GK, Darquenne C.** Effect of posture on regional deposition of coarse particles in the healthy human lung. *J Aerosol Med Pulm Drug Deliv* 28: 423–431, 2015. doi:10.1089/jamp.2014.1189.
29. **Simon BA, Kaczka DW, Bankier AA, Parraga G.** What can computed tomography and magnetic resonance imaging tell us about ventilation? *J Appl Physiol (1985)* 113: 647–657, 2012. doi:10.1152/japplphysiol.00353.2012.
30. **Svenningsen S, Guo F, Kirby M, Choy S, Wheatley A, McCormack DG, Parraga G.** Pulmonary functional magnetic resonance imaging: asthma temporal-spatial maps. *Acad Radiol* 21: 1402–1410, 2014. doi:10.1016/j.acra.2014.08.002.
31. **Venegas JG, Winkler T, Musch G, Vidal Melo MF, Layfield D, Tgavalekos N, Fischman AJ, Callahan RJ, Bellani G, Harris RS.** Self-organized patchiness in asthma as a prelude to catastrophic shifts. *Nature* 434: 777–782, 2005. doi:10.1038/nature03490.
32. **Winkler T, Venegas JG.** Complex airway behavior and paradoxical responses to bronchoprovocation. *J Appl Physiol (1985)* 103: 655–663, 2007. doi:10.1152/japplphysiol.00041.2007.
33. **Winkler T, Venegas JG, Harris RS.** Mathematical modeling of ventilation defects in asthma. *Drug Discov Today Dis Models* 15: 3–8, 2015. doi:10.1016/j.ddmod.2014.02.008.
34. **Yang G, Stewart CV, Sofka M, Tsai CL.** Registration of challenging image pairs: initialization, estimation, and decision. *IEEE Trans Pattern Anal Mach Intell* 29: 1973–1989, 2007. doi:10.1109/TPAMI.2007.1116.